

Preparation, characterization and electrochemical studies of 1,1'-bis(diphenylphosphino)ferrocene (dppf) derivatives. Crystal structure of [dppfCo(NO)₂][SbF₆]

Annelise E. Gerbase ^{a,*}, Eduardo J.S. Vichi ^b, Edison Stein ^b, Livio Amaral ^c,
Adalberto Vasquez ^c, Manfredo Hörner ^d, Cäcilia Maichle-Mössmer ^e

^a Instituto de Química, Universidade Federal do Rio Grande do Sul, Av. Bento Gonçalves 9500, 91501-970 Porto Alegre, RS, Brazil

^b Instituto de Química, Universidade Estadual de Campinas, Caixa Postal 6154, 13083-970 Campinas, SP, Brazil

^c Instituto de Física, Universidade Federal do Rio Grande do Sul, Av. Bento Gonçalves 9500, 91500 Porto Alegre, RS, Brazil

^d Departamento de Química, Universidade Federal de Santa Maria, 97119-900 Santa Maria, RS, Brazil

^e Institut für Anorganische Chemie, Universität Tübingen, Auf der Morgenstelle 18, D-72076 Tübingen, Germany

Received 5 September 1996; revised 18 October 1996; accepted 4 February 1997

Abstract

The neutral dppfFe(NO)₂ (1), the novel cationic [dppfCo(NO)₂][SbF₆] (2), as well as the dppfFe(CO)₃ (3) (dppf = 1,1'-bis(diphenylphosphino)ferrocene) complexes were prepared and characterized. The interaction between the two metallic centers through the dppf ligand was studied in the solid state by ⁵⁷Fe Mössbauer spectroscopy and in solution by cyclic voltammetry. The Mössbauer parameters are compared with those of other dppfML_n complexes. Electrochemical studies performed on these complexes show the great influence of the ML_n moiety on the redox processes of the dppf iron center. The crystal structure of complex 2 was determined (C₃₄H₂₈CoF₆FeN₂O₂P₂Sb). The compound crystallizes in the triclinic, space group *P*1̄, *a* = 10.441(2), *b* = 10.755(2), *c* = 17.320(5) Å, α = 104.10(2), β = 0.504(10), γ = 111.504(10)°, *U* = 1744.7(7) Å³, *Z* = 2, *R* = 0.0765, *wR*₂ = 0.1878. In this complex, the cobalt atom is coordinated to two nitrosyl ligands and to phosphorus atoms of the dppf ligand, providing a distorted tetrahedral geometry. © 1997 Elsevier Science S.A.

Keywords: Heterobimetallic complexes; Nitrosyl complexes; Cobalt complexes; Electrochemistry; Crystal structures

1. Introduction

An important part of organometallic chemistry has focused on the study of heterobimetallic compounds with the purpose of relating the possible interactions between the two metal atoms to the reactivity of the metallic centers in the molecule. In this sense, the two metal centers may act in a cooperative fashion to activate organic substrates.

The ferrocenyl ligands have been utilized to obtain such compounds, in particular, 1,1'-bis(diphenylphosphino)ferrocene (dppf). Many papers have been published recently describing the synthesis, solid state and solution characterization [1–11] of new metal derivatives of this compound as well as their catalytic properties [12–17].

⁵⁷Fe Mössbauer spectroscopy is a suitable technique for analyzing this metallo ligand containing an iron atom. The

technique provides structural information and shows eventual interactive effects between metallic centers, when the ligand complexes other metals.

Complexes that incorporate the dppf ligand are expected to exhibit a ferrocene-centered oxidative process, besides the redox processes due to other metallic centers present in the molecule. The study of the extent to which the former process is perturbed by the presence of either a second transition metal or the ligands attached to the metal is important, and may provide an insight into the ways of systematically tuning the redox potential of the ferrocene/ferricinium couple [18–21].

Nitrosyl complexes have been synthesized and characterized for a large number of transition metals [22,23]. Several metallic phosphino–nitrosyl complexes have been reported and their structures and reactivity have been extensively studied. Their catalytic activities in dimerization and oligomerization of olefins have been known for more than two decades [24–30]. Nevertheless, recently, the nitrosyl compounds

* Corresponding author.

have attracted considerable interest from the biological point of view due to the role of nitric oxide in vascular muscle relaxation [31].

The aim of this work is to describe the synthesis of bimetallic nitrosyls complexes with dppf, dppfFe(NO)_2 (**1**), $[\text{dppfCo(NO)}_2][\text{SbF}_6]$ (**2**) and dppfFe(CO)_3 (**3**), and to verify the existence of an interaction between the two metal atoms through the dppf ligand, in the solid state by ^{57}Fe Mössbauer spectroscopy at low temperature and in solution by studying the electrochemical behavior by cyclic voltammetry. The crystal structure of complex **2** was determined.

2. Experimental

2.1. General procedure

All the reactions were performed under argon using standard Schlenk techniques. dppf and AgSbF_6 were purchased from Strem and Aldrich, respectively, and were used without further purification. The complexes dppfFe(CO)_3 (**3**), dppeFe(NO)_2 (**4**), $[\text{dppeCo(NO)}_2][\text{SbF}_6]$ (**5**), dppeFe(CO)_3 (**6**) (dppe = 1,1'-bis(diphenylphosphino)ethane), $[\text{Co(NO)}_2\text{Cl}]_2$ and $[\text{Fe(NO)}_2\text{Cl}]_2$, were prepared following the methods described elsewhere [2,18,32–36]. The reagent grade solvents were dried by standard procedures and freshly distilled or degassed with argon before use.

2.2. Preparations

2.2.1. dppfFe(NO)_2 (**1**)

A solution of dppf (554 mg, 1 mmol) in 10 ml CH_2Cl_2 was added to a solution of $[\text{Fe(NO)}_2\text{Cl}]_2$ (151 mg, 0.5 mmol) and Zn (327 mg, 5 mmol) in 10 ml of CH_2Cl_2 . The mixture was stirred for 3 h at room temperature. The excess of metallic Zn was filtered off and the solution was concentrated to 1 ml. The product crystallizes as brown crystals on cooling after addition of hexane. Yield of crude product: 70%. *Anal. Calc.* for $\text{C}_{34}\text{H}_{28}\text{N}_2\text{O}_2\text{P}_2\text{Fe}_2$: C, 60.89; H, 4.18; N, 4.18. Found: C, 59.47; H, 4.12; N, 4.18%. IR (CH_2Cl_2): $\nu\text{NO} = 1710$ and 1660 cm^{-1} . $^1\text{H NMR}$ (CDCl_3): $\delta = 4.24$ (m, 8H), 7.20–7.60 (m, 20H). $^{31}\text{P}\{^1\text{H}\}$ NMR (CDCl_3): $\delta = 57.87$.

2.2.2. $[\text{dppfCo(NO)}_2][\text{SbF}_6]$ (**2**)

A solution of AgSbF_6 (343 mg, 1 mmol) in 100 ml acetonitrile was added to a solution of $[\text{Co(NO)}_2\text{Cl}]_2$ (95 mg, 0.5 mmol) in 10 ml acetonitrile. The mixture was stirred at room temperature. After 2 h, the AgCl precipitate was removed by filtration. A solution of dppf (554 mg, 1 mmol) in 10 ml acetonitrile was added to the filtrate and stirred at room temperature for 2 h. The solution was concentrated to 1 ml and 20 ml hexane were added at low temperature. The final product was filtered off, washed with hexane and dried under vacuum. Yield of crude product: 71%. *Anal. Calc.* for

$\text{C}_{34}\text{H}_{28}\text{N}_2\text{O}_2\text{P}_2\text{F}_6\text{FeCoSb}$: C, 44.93; H, 3.08; N, 3.08. Found: C, 44.80; H, 2.44; N, 2.96%. IR (CH_2Cl_2): $\nu\text{NO} = 1850$ and 1798 cm^{-1} . $^1\text{H NMR}$ (CDCl_3): $\delta = 4.43$ (s, 4H), 4.63 (s, 4H), 7.30–7.55 (m, 20H). $^{31}\text{P}\{^1\text{H}\}$ NMR (CDCl_3): $\delta = 47.36$. Λ_M (acetone, 25°C): $149\text{ S cm}^2\text{ mol}^{-1}$.

2.3. Spectral measurements

Elemental analyses were performed on a Perkin-Elmer CHN 2400 apparatus.

The Mössbauer spectra were recorded on a conventional constant acceleration Mössbauer spectrometer. The source was ^{57}Co in an Rh matrix with a nominal activity of 50 mCi. All isomer shifts are compared to metallic iron at room temperature. The measurements were performed in a horizontal geometry at liquid nitrogen temperature. The experimental data were fitted by a simple least-squares procedure. Typical standard deviation for the Mössbauer parameters fitting is 0.001 mm s^{-1} .

IR spectra were recorded on a Perkin-Elmer 1430 spectrophotometer using NaCl liquid cells with 0.15 mm of optical pathway.

The $^1\text{H NMR}$ and $^{31}\text{P}\{^1\text{H}\}$ NMR spectra were obtained on a Varian VXR200 spectrometer operating at 200 and 80.89 MHz, respectively, at room temperature, using CDCl_3 or CH_2Cl_2 as solvent. All chemical shifts are in ppm, relative to TMS or 85% H_3PO_4 , using the positive downfield convention.

2.4. Electrochemical measurements

Electrochemical measurements were performed in an EG&G Princeton Applied Research (PAR) M270 electrochemical analyzer interfaced to an IBM computer employing a PAR Electrochemical Software. A standard three-electrode cell was designed allowing that the tip of the reference electrode closely approaches the working electrode. Positive feedback iR compensation was applied routinely. All measurements were carried out under argon in anhydrous deoxygenated dichloroethane; solutions were $\sim 4 \times 10^{-3}\text{ M}$ in the supporting electrolyte, $[\text{Bu}_4\text{N}][\text{BF}_4]$. A platinum-disk working electrode and a saturated calomel electrode (SCE) were used in these experiments. Potential data are relative to ferrocene as internal standard. Under the experimental conditions the ferrocene/ferrocenium couple is located at +0.57 versus SCE.

2.5. Molecular structure of $[\text{ddpfCo(NO)}_2][\text{SbF}_6]$ (**2**)

The crystal structure of **2** was determined using a monocrystal obtained by slow diffusion of a toluene layer into a solution of the complex in 1,2-dichloroethane at 10°C , under argon atmosphere.

Table 1 summarizes the crystal data and structure refinement parameters for **2**. Diffractometric intensity data were collected at 223(2) K on an automatic four circle diffracto-

Table 1

Crystal data and structure refinement for [dppfCo(NO)₂][SbF₆], with e.s.d.s in parentheses

Empirical formula	C ₃₄ H ₂₈ CoF ₆ FeN ₂ O ₂ P ₂ Sb
Formula weight	909.05
Temperature (K)	223(2)
Wavelength (Å)	1.54056
Crystal system	triclinic
Space group	P $\bar{1}$
Unit cell dimensions	
<i>a</i> (Å)	10.441(2)
<i>b</i> (Å)	10.755(2)
<i>c</i> (Å)	17.320(5)
α (°)	104.10(2)
β (°)	90.504(10)
γ (°)	111.504(10)
Volume (Å ³), <i>Z</i>	1744.7(7), 2
Density (calc.) (Mg m ⁻³)	1.730
Absorption coefficient (mm ⁻¹)	14.522
<i>F</i> (000)	656
Crystal size (mm)/color	0.25 × 0.05 × 0.05/black
No. reflections (lattice)	25
θ Range (lattice) (°)	9.3–23.6
θ Range for data collection (°)	5.03–67.19
Limiting indices	–1 ≤ <i>h</i> ≤ 12, –12 ≤ <i>k</i> ≤ 12, –20 ≤ <i>l</i> ≤ 20
Reflections collected	7292
Independent reflections	6188 (<i>R</i> (int) = 0.0562)
Reflections observed	3129
Criterion for observation	(<i>I</i> > 2 σ (<i>I</i>))
Absorption correction	DIFABS
Max. and min. transmission	1.317 and 0.798
Refinement method	full-matrix least-squares on <i>F</i> ²
Data/restraints/parameters	6188/0/443
Goodness-of-fit on <i>F</i> ²	1.012
Final <i>R</i> indices (<i>I</i> > 2 σ (<i>I</i>))	<i>R</i> ₁ = 0.0765, <i>wR</i> ₂ = 0.1878 <i>w</i> = 1/[$\sigma^2(F_o^2) + (0.1305P)^2 + 3.7853P$] where <i>P</i> = (<i>F_o</i> ² + 2 <i>F_c</i> ²)/3
Maximal (Δ/σ)	0.005
Extinction coefficient	0.0013(2)
Largest difference peak and hole (e Å ⁻³)	0.942 and –1.619

meter with kappa geometry (Enraf-Nonius CAD4) [37] using graphite-monochromated Cu K α radiation and ω -2 θ scans with a scan speed of 45 s/reflection. In intervals of ∞ min the orientation of the crystal was controlled by three standard reflections and no appreciable intensity loss was observed during the data collection. The structure was solved using the direct methods employing the VAXSDP [38] and SHELXS86 [39] programs and all non-hydrogen atoms were located by subsequent Fourier difference synthesis. All non-hydrogen atoms were refined employing the SHELXL93 program [40] using anisotropic thermal parameters. The positions of the hydrogen atoms were calculated based on the geometry of the molecule and the thermal displacement parameters were refined isotropically on a groupwise basis [41]. Scattering factors for all atoms were as in the SHELXL93 [40] program.

3. Results and discussion

The preparation of the nitrosyl compounds was carried out following similar methods used to prepare other iron and cobalt nitrosyl compounds [18,34].

The reaction between 1,1'-bis(diphenylphosphino)-ferrocene (dppf) and [Fe(NO)₂Cl]₂, in CH₂Cl₂, in the presence of powdered metallic Zn yield the bimetallic complex dppfFe(NO)₂ (1). The compound was characterized by ¹H and ³¹P NMR, IR and elemental analysis. The resulting data agree very well with those reported by Munyejabo et al. [11].

When [Co(NO)₂Cl]₂ reacts with AgSbF₆ in the presence of a solvent like acetonitrile, the dimer structure is disrupted and AgCl precipitation occurs. The addition of a dppf solution to the cobalt solution yields the formation of the new bimetallic compound 2. The IR spectrum shows two linear NO

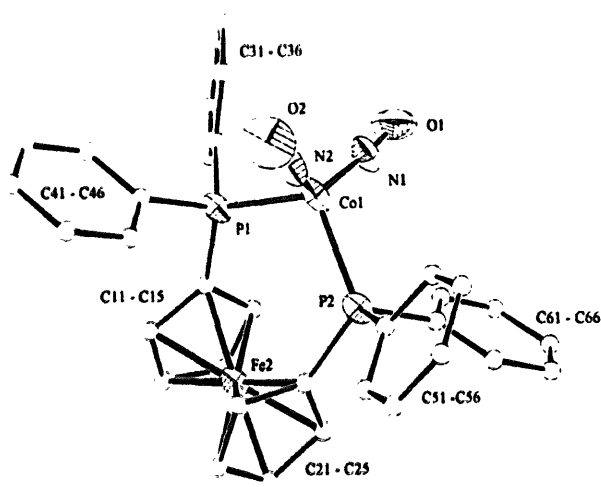


Fig. 1. ORTEP [46] plot with atom-labeling scheme of the structure of the cation of $[\text{dppfCo}(\text{NO})_2][\text{SbF}_6]$ (**2**), displacement ellipsoids at the 50% level; H atoms omitted for clarity.

stretching frequencies, at 1850 and 1798 cm^{-1} , characteristic for the cationic cobalt dinitrosyl moiety bonded to phosphine ligands [42], as well as the frequencies related to the ferrocenyl ligand [43]. The $^3\text{P}\{^1\text{H}\}$ NMR spectrum shows only one singlet, at 47.36 ppm, shifted downfield when compared to the free dppf singlet at -16.5 ppm [44], which is typical for diphosphines bonded to a metal as bidentate ligand [45].

3.1. Crystal structure of **2**

An ORTEP [46] drawing of the structure of the cation of **2** is shown in Fig. 1. Atomic positional parameters for non-hydrogen atoms are listed in Table 2 and selected bond distances and bond angles are presented in Table 3. In this complex, dppf functions as a chelating ligand. The geometry of the cobalt nitrosyl moiety in **2** is that of a distorted tetrahedron. The cobalt atom is coordinated to two nearly linear nitrosyl ligands ($173.2(12)$ and $175.3(13)^\circ$) and to the two phosphorus donors of dppf. The $\text{Co}(\text{NO})_2$ group is planar. The $\text{Co}=\text{N}$ and $\text{N}=\text{O}$ bond lengths and $\text{N}=\text{Co}=\text{N}$ and $\text{Co}=\text{N}=\text{O}$ angles are close to those found in other cobalt dinitrosyl complexes containing linearly coordinated NO groups [47].

Extensive studies on metal complexes containing substituted ferrocenyl phosphine ligands exhibit quite large $\text{P}=\text{M}=\text{P}$ angles for a bidentate diphosphine. The same trend is observed for compound **2**. The $\text{P}=\text{Co}=\text{P}$ angle of $106.17(13)^\circ$ is large in comparison with the 87.8° observed in the analogous diphosphine derivative $[\text{dppeCo}(\text{NO})_2]^+$ [48,49], but very close to the angle of 106.7° presented in the PPh_3 derivative [50], which is a non-bidentate phosphine.

The Cp rings are planar within experimental error and all structural parameters related to the PF_6^- group are found in the expected ranges (see Table 3) and show no disordering.

3.2. Mössbauer studies

Mössbauer data of **1** were fitted with two doublets corresponding to two iron sites, A and B, as shown in Table 4 and

Table 2

Atomic coordinates ($\times 10^4$) and equivalent isotropic displacement parameters ($\text{\AA}^2 \times 10^3$) for $[\text{dppfCo}(\text{NO})_2][\text{SbF}_6]$, with e.s.d.s in parentheses

	x	y	z	U_{eq}
Co(1)	11199(2)	10522(2)	8127(1)	52(1)
Fe(2)	9389(2)	12989(2)	7293(1)	49(1)
P(1)	10718(3)	10427(3)	6825(2)	48(1)
P(2)	10705(3)	12335(3)	8884(2)	50(1)
Sb(1)	4441(1)	7272(1)	7007(1)	71(1)
F(1)	4366(10)	6033(12)	7595(7)	128(4)
F(2)	2757(12)	6058(15)	6488(7)	149(5)
F(3)	4520(17)	8479(16)	6410(10)	185(6)
F(4)	6143(14)	8384(14)	7529(8)	182(6)
F(5)	3515(19)	8042(13)	7742(9)	204(8)
F(6)	5236(14)	6433(15)	6209(8)	163(5)
O(1)	9195(13)	7991(11)	8180(8)	101(4)
O(2)	14052(11)	11304(13)	8292(8)	111(4)
N(1)	10023(13)	9059(12)	8205(7)	66(3)
N(2)	12887(13)	11002(12)	8257(7)	67(3)
C(11)	9553(12)	11223(11)	6602(8)	51(3)
C(12)	9782(14)	12238(11)	6162(8)	56(3)
C(13)	8584(15)	12536(13)	6126(8)	62(4)
C(14)	7610(14)	11752(13)	6549(9)	63(4)
C(15)	8205(12)	10938(12)	6855(8)	52(3)
C(21)	10301(13)	13500(11)	8422(8)	54(3)
C(22)	11162(13)	14368(12)	7971(8)	55(3)
C(23)	10380(15)	15107(12)	7728(8)	61(4)
C(24)	9103(16)	14690(13)	7997(9)	65(4)
C(25)	9006(13)	13684(12)	8436(8)	55(3)
C(31)	9860(13)	8624(12)	6258(7)	48(3)
C(32)	10526(14)	7716(13)	6302(8)	60(4)
C(33)	9880(17)	6341(13)	5901(9)	71(4)
C(34)	8594(15)	5830(12)	5471(8)	62(4)
C(35)	7975(13)	6737(12)	5418(8)	58(3)
C(36)	8598(14)	8134(13)	5825(8)	59(3)
C(41)	12261(12)	11149(12)	6376(7)	48(3)
C(42)	12541(14)	10429(14)	5646(9)	63(4)
C(43)	13754(15)	11016(18)	5310(10)	77(4)
C(44)	14669(15)	12316(17)	5657(10)	72(4)
C(45)	14413(15)	13025(16)	6383(11)	80(5)
C(46)	13240(14)	12466(13)	6745(10)	69(4)
C(51)	12106(13)	13442(12)	9665(8)	53(3)
C(52)	12649(13)	14874(13)	9826(8)	58(3)
C(53)	13652(13)	15677(14)	10465(9)	67(4)
C(54)	14123(14)	15049(16)	10938(9)	71(4)
C(55)	13602(15)	13595(18)	10789(9)	78(4)
C(56)	12600(13)	12823(15)	10154(8)	64(4)
C(61)	9226(12)	11734(12)	9419(7)	48(3)
C(62)	8046(12)	10617(12)	9061(8)	56(3)
C(63)	6894(14)	10184(15)	9444(10)	69(4)
C(64)	6898(15)	10865(14)	10229(10)	69(4)
C(65)	8026(15)	11982(14)	10617(9)	68(4)
C(66)	9194(13)	12429(13)	10222(8)	59(3)

U_{eq} is defined as one third of the trace of the orthogonalized U_{ij} tensor.

Fig. 2(A), in the same proportion, but in quite different environments. Site A was assigned to the ferrocenyl iron atom since the values of the parameters $\text{IS} = 0.52 \text{ mm s}^{-1}$ and $\text{QS} = 2.34 \text{ mm s}^{-1}$ correspond to an iron site in a high oxidation state and a non-symmetrical geometry. The values obtained agree with those for the free ligand, $\text{IS} = 0.53 \text{ mm s}^{-1}$ and $\text{QS} = 2.30 \text{ mm s}^{-1}$, and related metal complexes

Table 3
Selected bond lengths (Å) and angles (°) for [dppfCo(NO)₂][SbF₆], with e.s.d.s in parentheses

Co(1)–N(2)	1.641(13)
Co(1)–N(1)	1.641(13)
Co(1)–P(1)	2.275(4)
Co(1)–P(2)	2.300(4)
Fe(2)–C(21)	2.023(13)
Fe(2)–C(11)	2.049(11)
P(1)–C(41)	1.790(13)
P(1)–C(11)	1.811(11)
P(1)–C(31)	1.820(12)
P(2)–C(61)	1.802(13)
P(2)–C(21)	1.805(12)
P(2)–C(51)	1.814(13)
Sb(1)–F(4)	1.815(12)
Sb(1)–F(5)	1.826(11)
Sb(1)–F(3)	1.827(13)
Sb(1)–F(2)	1.822(12)
Sb(1)–F(6)	1.837(11)
Sb(1)–F(1)	1.845(10)
O(1)–N(1)	1.147(14)
O(2)–N(2)	1.135(14)
N(2)–Co(1)–N(1)	127.2(6)
N(2)–Co(1)–P(1)	104.9(4)
N(1)–Co(1)–P(1)	101.6(4)
N(2)–Co(1)–P(2)	106.3(4)
N(1)–Co(1)–P(2)	108.9(4)
P(1)–Co(1)–P(2)	106.17(13)
C(41)–P(1)–C(11)	106.5(5)
C(41)–P(1)–C(31)	107.1(6)
C(11)–P(1)–C(31)	103.4(5)
C(41)–P(1)–Co(1)	111.7(4)
C(11)–P(1)–Co(1)	118.1(4)
C(31)–P(1)–Co(1)	109.2(4)
C(61)–P(2)–C(21)	102.6(6)
C(61)–P(2)–C(51)	104.2(6)
C(21)–P(2)–C(51)	105.2(6)
C(61)–P(2)–Co(1)	111.5(4)
C(21)–P(2)–Co(1)	120.9(4)
C(51)–P(2)–Co(1)	110.9(4)
F(4)–Sb(1)–F(5)	94.4(8)
F(4)–Sb(1)–F(3)	91.5(7)
F(5)–Sb(1)–F(3)	91.5(7)
F(4)–Sb(1)–F(2)	176.3(7)
F(5)–Sb(1)–F(2)	87.6(7)
F(3)–Sb(1)–F(2)	91.6(7)
F(4)–Sb(1)–F(6)	90.2(7)
F(5)–Sb(1)–F(6)	175.2(8)
F(3)–Sb(1)–F(6)	87.0(7)
F(2)–Sb(1)–F(6)	87.9(6)
F(4)–Sb(1)–F(1)	88.8(6)
F(5)–Sb(1)–F(1)	89.3(6)
F(3)–Sb(1)–F(1)	179.1(6)
F(2)–Sb(1)–F(1)	88.1(5)
F(6)–Sb(1)–F(1)	92.1(6)
O(1)–N(1)–Co(1)	173.2(12)
O(2)–N(2)–Co(1)	175.3(13)
P(1)–C(11)–Fe(2)	126.6(6)
P(2)–C(21)–Fe(2)	125.2(6)

[44,51]. The parameters IS and QS from site B, 0.07 and 0.64 mm s⁻¹, typical for a site in a low oxidation state and a very symmetrical arrangement, are close to the ones obtained

for dppfFe(NO)₂, IS = 0.03 mm s⁻¹ and QS = 0.54 mm s⁻¹, and for Fe(NO)₂(PPh₃)₂, IS = 0.09 mm s⁻¹ and QS = 0.68 mm s⁻¹ [52,53]. Site B was assigned to an iron tetrahedrally bonded to two linear nitrosyls, at one side, and to the P atoms of the ferrocenyl ligand, at the other.

The Mössbauer data of **2**, Fig. 2(B), were fitted with one doublet, with IS = 0.52 mm s⁻¹ and QS = 2.30 mm s⁻¹, assigned to the iron ferrocenyl atom [44,51].

The Mössbauer spectrum of **3**, displayed in Fig. 2(C), shows two iron sites, A and B, in the same proportion. The values of the parameters for site A, IS = 0.51 mm s⁻¹ and QS = 2.33 mm s⁻¹, agree with the ones for the iron dppf ligand, and the values for site B, IS = -0.05 mm s⁻¹ and QS = 2.18 mm s⁻¹, characteristic for a site in a low oxidation state and a non-symmetrical geometry, are close to those for dppcFe(CO)₃, IS = -0.098 mm s⁻¹ and QS = 2.76 mm s⁻¹, and Fe(CO)₃(PPh₃)₂, IS = -0.072 mm s⁻¹ and QS = 2.12 mm s⁻¹, and were assigned to the iron atom of the Fe(CO)₃ moiety [54].

The values of the site A parameters show no direct interaction between the two metal atoms. The QS value is significantly smaller than 3.00 mm s⁻¹ that might be expected for such interactions, as in Hg adducts [51].

The iron ferrocenyl Mössbauer data of the complexes obtained in this work are in the range of those for related transition metal complexes (IS = 0.50–0.58 mm s⁻¹ and QS = 2.14–2.39 mm s⁻¹) [44,51].

Corain et al. [44] measured the hyperfine parameters of a series of metal halide complexes of dppf. They did not find any relationship between them and the electronegativity or ionic/covalent radii of the coordinated metal.

Houlton et al. [51] reported Mössbauer data for a series of dppf metal halide and carbonyl complexes. According to these authors, the distortion of the ferrocenyl moiety is caused by the coordination geometry of the metal which influences the hyperfine interactions of the ferrocenyl iron atom. In an IS versus QS plot, they found that the highest IS (0.55–0.58) and QS (2.29–2.36) values are those for the tetrahedral complexes (dppfMX₂, where M = Ni, Fe, Zn, Hg, Co; X = Cl, Br, I). The lowest IS (0.50–0.51) and QS (2.14–2.29) parameters correspond to the square planar complexes (dppfMCl₂, where M = Pd, Pt, Cd). Finally, the octahedral complexes (dppfM(CO)₄, where M = Cr, Mo, W) have intermediate values, IS (0.52–0.54) and QS (2.23–2.27).

The crystal structure of compound **1** shows that the iron atom bonded to dppf possesses a tetrahedral geometry [11]. The same was observed by us for the Co atom in compound **2**, as described above. Thus, the Mössbauer parameters of compounds **1** and **2** are expected to coincide with those obtained for the tetrahedral dppfMCl₂ complexes. However, this coincidence has not been observed. On the other hand, the hyperfine parameters of complex **3**, which has distorted trigonal bipyramid local symmetry around the iron atom of the 'Fe(CO)₃' moiety [9], are closely related to the ones obtained for the iron and cobalt dinitrosyls, and Cr, Mo and W tetracarbonyls. Thus, it seems that electronic effects of

Table 4
Mössbauer data

Compounds	Mössbauer parameters ^a (mm s ⁻¹)				Ref.
	Sites	IS	QS	Γ	
dppf	A	0.53	2.33		[51]
dppfFe(NO) ₂ (1)	A	0.52	2.34	0.26	^b
	B	0.07	0.64	0.26	
[dppfCo(NO) ₂][SbF ₆] (2)	A	0.52	2.30	0.26	^b
dppfFe(CO) ₃ (3)	A	0.51	2.33	0.25	^b
	B	-0.05	2.18	0.27	

^a Measurements performed at 77 K, IS = isomer shift referred to a metal iron at room temperature as zero shift, QS = quadrupole splitting, Γ = linewidth.

^b This work.

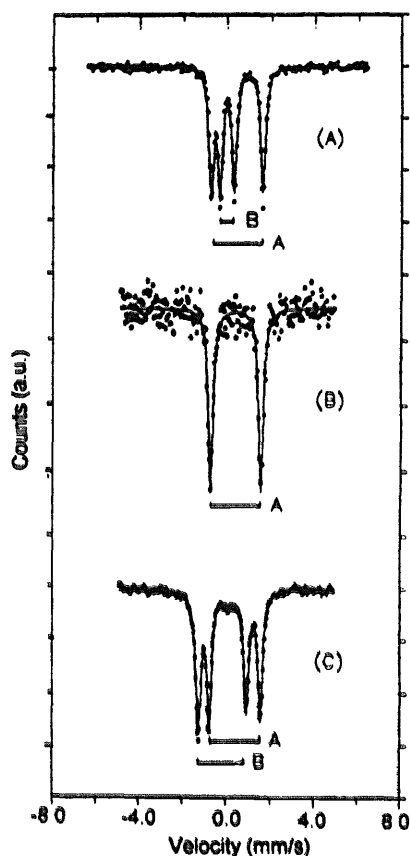


Fig. 2. Mössbauer spectra of the complexes (A) dppfFe(NO)₂ (1), (B) [dppfCo(NO)₂][SbF₆] (2) and (C) dppfFe(CO)₃ (3).

ligands that are powerful π -acceptors, such as CO and NO⁺, influence the iron atom in the dppf moiety quite differently to the σ - and π -donors in the halide series.

Although small our results show that the influence of the ML_n moiety on the hyperfine parameters of the ferrocenyl site is not purely steric and depends on the electronic properties of the ML_n fragment.

3.3. Electrochemical measurements

The relevant electrochemical data for complexes dppfFe(NO)₂ (1), [dppfCo(NO)₂]⁺ (2) and dppfFe(CO)₃ (3), for the free ligand dppf, and for the complexes dppeFe(NO)₂

Table 5
Voltammetric data of dppf derivatives^a

Compound	$E_{1/2}$ (V vs. SCE)	ΔE (mV)
Ferrocene	0.57	74
dppf	0.76	77
dppfFe(NO) ₂ (1)	0.487	79
	1.386 ^b	
dppeFe(NO) ₂ (4)	0.497	95
[dppfCo(NO) ₂][SbF ₆] (2)	-0.390	92
	1.193	86
[dppeCo(NO) ₂][SbF ₆] (5) ^c	-0.408	130
	2.00 ^b	
dppfFe(CO) ₃ (3)	0.396	88
	0.541	78
	1.900 ^b	
dppeFe(CO) ₃ (6)	0.214	77
	1.53 ^b	

^a Platinum electrode (saturated calomel electrode, SCE, as standard). Dichloroethane solutions with 0.1 M [n-Bu₄N][BF₄]. $E_{1/2}$ halfwave potential (V). ΔE = peak separation between anodic and cathodic peak potential (mV). Scan rate = 200 mV s⁻¹.

^b E_p = anodic peak potential (V).

^c Scan rate = 150 mV s⁻¹.

(4), [dppeCo(NO)₂][SbF₆] (5) and dppeFe(CO)₃ (6), where dppe is 1,2-bis(diphenylphosphino)ethane, are given in Table 5. Complexes 4, 5 and 6 were prepared and analyzed for comparison purposes.

The anodic scan of a compound 1 solution shows two distinct processes, only the first one displaying a directly associated reduction peak. The first couple, $E_{1/2} = 0.487$ V versus SCE, corresponds to a one-electron transfer quasi-reversible process, since the E versus $\log[(i_d - i)/i]$ plot, obtained from normal pulse voltammetry data, is linear throughout the origin, with a slope of 69 mV, indicating a Nernstian process. It was assigned to an oxidation of the iron atom bonded to the nitrosyl groups since the cyclic voltammogram of the analog compound, dppeFe(NO)₂ (4), exhibits an oxidation couple at $E_{1/2} = 0.497$ V versus SCE and no other oxidation process. The second oxidation peak B, at $E_p = 1.386$ V versus SCE, corresponds to an irreversible one-electron transfer process, which was assigned to the oxidation of the ferrocenyl ligand.

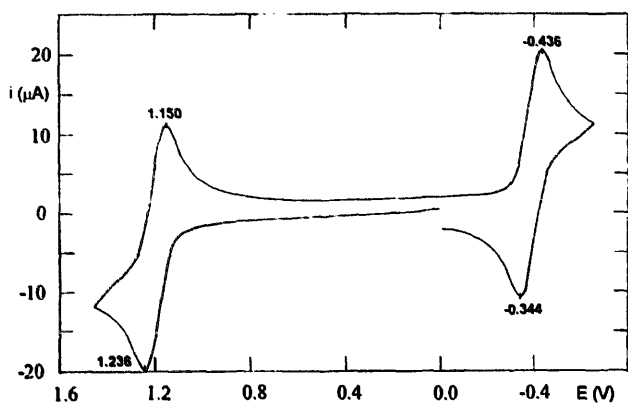


Fig. 3. Cyclic voltammogram for the complexes $[\text{dppfCo}(\text{NO})_2][\text{SbF}_6]$ (**2**) measured at 200 mV s^{-1} in dichloroethane/ 0.1 M $[\text{n-Bu}_4\text{N}][\text{BF}_4]$ using a Pt vs. SCE at 25°C .

Fig. 3 shows the cathodic and anodic responses of compound **2**. In the cathodic scan this compound exhibits a quasi-reversible peak at $E_{1/2} = -0.390 \text{ V}$ versus SCE, corresponding to the reduction of the cationic complex. A linear plot E versus $\log[(i_d - i)/i]$ with a slope of 60 mV was obtained from normal pulse voltammetry data, indicating a Nernstian process of one electron transfer. In the anodic scan a quasi-reversible oxidation process was observed, $E_{1/2} = 1.193 \text{ V}$ versus SCE, corresponding to a one-electron transfer process. This peak was assigned to the oxidation of the iron atom of the ferrocenyl ligand. The cyclic voltammogram of the analog compound $[\text{dppeCo}(\text{NO})_2][\text{SbF}_6]$ (**5**) did not show any peak in this region. It exhibits an irreversible anodic peak very close to the solvent discharge, probably due to the formation of very unstable oxidized phosphine species and a quasi-reversible cathodic peak with $E_{1/2} = -0.408 \text{ V}$ versus SCE. Seeber et al. [55] observed a similar peak, $E_{1/2} = -0.390 \text{ V}$ versus SCE, for the complex $\{[\text{P}(\text{OEt})_3]_2\text{Co}(\text{NO})_2\}[\text{BF}_4]$, assigned to the reduction of the central metal.

The cyclic voltammogram of compound **3** shows three oxidation processes. The first two quasi-reversible peaks, $E_{1/2} = 0.396 \text{ V}$ and $E_{1/2} = 0.541 \text{ V}$ versus SCE, are related to one-electron transfer processes. In sampled d.c. polarography, two well-resolved waves are observed in the range $0.20\text{--}0.70 \text{ V}$, with half-peak potentials $E_{1/2} = 0.395$ and 0.540 V , respectively. Both E versus $\log[(i_d - i)/i]$ plots are linear throughout the origin with slopes of 59 and 60 mV , respectively, indicating two Nernstian one-electron processes. The square peak voltammetry (SWV) response of a dichloroethane complex solution in the frequency range $30\text{--}90 \text{ Hz}$, having E_{sw} of 0.395 and 0.539 V versus SCE is illustrated in Fig. 4. The plots of i_{sw} versus the square root of the frequency are linear throughout the origin for both oxidation processes. The wave widths, $w_{1/2}$ (~ 108 and 109 mV , respectively) are independent of the frequency and close to the value expected for a Nernstian one-electron process (99 mV at 25°C) [56,57].

Indications that a multielectronic oxidation process occurs on the iron bonded to the carbonyls, are: (i) the potential

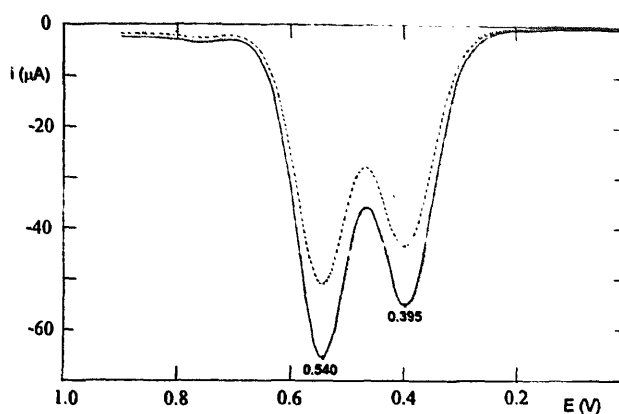


Fig. 4. Square peak voltammetry response of a $\text{C}_2\text{H}_4\text{Cl}_2$ solution at room temperature of $\text{dppfFe}(\text{CO})_3$ (**3**). The frequencies employed were: \cdots , 30; $-\cdot-$, 60; $—$, 90 Hz.

peaks separation of 145 mV [58]; (ii) the potential values lower than the ones obtained for the free dppf ligand; (iii) the two oxidation processes of one electron each obtained from the polarogram and SWV curves. The metal, formally in a zero oxidation state, oxidizes stepwise in a two-electron process, forming very unstable species. The third oxidation process in complex **3**, $E_p = 1.900 \text{ V}$ versus SCE, with irreversible character, and a signal very close to the solvent discharge, can be assigned either to the oxidation of the iron in the ferrocenyl ligand or to the formation of very unstable oxidized phosphine species.

The electrochemical formation of iron carbonyl species in unusual oxidation states for the dppf derivative was not observed for other analog carbonyl complexes. The one-electron oxidation of iron carbonyl compounds $\text{L}_2\text{Fe}(\text{CO})_3$ and $\text{LFe}(\text{CO})_4$, where $\text{L} = \text{phosphines, arsine or stibine}$, is dependent on the solvent and working electrode [59]. Complexes $\text{L}_2\text{Fe}(\text{CO})_3$, where $\text{L} = \text{PPh}_3, \text{AsPh}_3, \text{PMePh}_2, \text{P}(\text{NMe})_3, \text{P}(\text{OPh})_3, 1/2 \text{ dppe}$ and $1/2 \text{ dppm}$ (diphenylphosphinomethane), undergo one-electron oxidation to monocationic compounds at the Pt electrode [60]. Generally, the oxidation process is reversible and exhibits anodic potential peaks between 0.33 and 0.12 V versus SCE with a marked dependence of $E_{1/2}$ on the nature of L ; an increase in the basicity of the ligand results in a shift of $E_{1/2}$ to a more negative potential.

The same effect is observed comparing compounds **3** and **6**. However, it is not observed for compounds **1** and **4**, and **2** and **5**, where the differences in the oxidation/reduction potentials are too small to be considered. A possible explanation for the different behavior of the iron carbonyl complexes (**3** and **6**), compared to the iron (**1** and **4**) and cobalt nitrosyl complexes (**2** and **5**), is that small variations in the charge on the metal atoms, due to an increase in the basicity of ligands L , are buffered by the nitrosyl ligand, since NO^+ is a stronger π -acceptor than CO [61].

This effect could also explain why dppf induces a multielectronic oxidation process on the iron carbonyl in complex **3**, and why the same is not observed for the nitrosyl compound

1. Since the CO ligand is a weaker π -acceptor than the NO^+ ligand, the electron density on the iron atom in complex **3** is greater than in complex **1**, and consequently, the oxidation process is easier in the former complex, allowing the stepwise oxidation of the iron atom.

With $\text{L} = \text{PPh}_3$, it was possible to synthesize the cation $[(\text{PPh}_3)_2\text{Fe}(\text{CO})_3][\text{PF}_6]$, and its cyclic voltammogram shows a one-electron reduction at an identical potential to the oxidation of the neutral complex [62]. Nevertheless with $\text{L} = \text{dppe}$, the $\text{dppeFe}(\text{CO})_3$ complex undergoes a chemical oxidation with NH_4PF_6 or AgPF_6 , but the formed cationic species are unstable and are only detected in solution by IR. In fact, the complex $\text{dppeFe}(\text{CO})_3$ (**6**) undergoes, under our experimental conditions, a quasi-reversible one-electron oxidation process at $E_{1/2} = 0.214$ V versus SCE attributed to the oxidation of the iron atom, and an irreversible peak at $E_p = 1.53$ V versus SCE ascribed to a phosphine oxidation.

In general, when the dppf ligand is coordinated to transition metals, the oxidation becomes more difficult, and the found potentials are more anodic than the free ligand [44,63–67]. The complexes studied in this work present a ferrocene-based oxidation potential more anodic than that of the free ligand. In the case of the iron derivatives **1** and **3**, the oxidation of the dppf moiety leads to very unstable cationic species and irreversible processes were observed. For the cationic complex **2**, the oxidation shows a reversible behavior, i.e. the oxidized species formed is probably stabilized by the presence of a stronger π -acceptor ligand, NO^+ . The oxidation potential depends on the transition metal coordinated to dppf and to the nature of the other ligands. Corain et al. [44] compared the voltammetric behavior of the halide complexes dppfMCl_2 . With $\text{M} = \text{Pt}$, Pd , the resulting voltammograms show a reversible oxidation peak; with $\text{M} = \text{Co}$, Ni , Zn , Cd , Hg , the complexes exhibit irreversible or ill-defined anodic peaks. In the case of the square-planar complexes of $\text{Pt}(\text{II})$ and $\text{Pd}(\text{II})$, this different behavior was explained by the back-donation that reinforces the $\text{P}-\text{M}$ bond and stabilizes the formed oxidation species, $[\text{dppfMCl}_2]^+$.

The analysis of the cyclic voltammogram relative to the oxidation/reduction of the central iron atom of the complexes studied in this work (with a scan rate varying from 0.2 to 1.0 V s^{-1}), confirms that the one-electron removal/addition is not accompanied by subsequent chemical reactions. The ratio $i_{pa}/i_{pc} < 1$, remains constant, the product $i_p \nu^{-1/2}$ is substantially constant and the peak-to-peak separation increases progressively. The departure of this last parameter from the value of 59 mV, expected for an electrochemically reversible electron transfer, may be attributed to reorganization within the complexes and/or the solvent, which raises the barrier for electron transfer slowing down the relative rate, and also to an uncompensated solution resistance. Under the present experimental conditions, the one-electron oxidation of ferrocene is known to involve minimal structural reorganization [68–70] and displays a similar trend of ΔE_p with scan rate. Thus, the removal/addition of one electron from the studied complex should also cause minimal geometrical rearrange-

ment [71]. The ratio $i_{pa}/i_{pc} < 1$ remains constant with increasing scan rate. This behavior can account for the instability of electrogenerated complexes formed after oxidation/reduction under the experimental conditions.

4. Conclusions

In this work, the $\text{dppfFe}(\text{NO})_2$ (**1**), the new cationic $[\text{dppfCo}(\text{NO})_2][\text{SbF}_6]$ (**2**) and the $\text{dppfFe}(\text{CO})_3$ (**3**) complexes were prepared, characterized and the molecular structure of **2** was determined. The small changes observed in the Mössbauer parameters are comparable with those of similar compounds and suggest that there is a weak interaction between the two metallic atoms through the dppf ligand, in the solid state, at low temperature. Two main features emerge from the electrochemical studies of complexes **1**, **2** and **3**. Firstly, in solution, the ML_n coordination has a great influence on the iron dppf oxidation process. In general, it causes a more difficult oxidation process and can modify the oxidation mechanism. Secondly it was possible to generate, in solution, species, with very unusual oxidation states.

Acknowledgements

Supplementary information is available from the authors on request. The authors thank the CNPq, FAPERGS, Stiftung Volkswagenwerk, and CAPES/DAAD (PROBRAL) for financial support.

References

- [1] T.S. Andy Hor and L.-T. Phang, *J. Organomet. Chem.*, **390** (1990) 345.
- [2] T.S. Andy Hor and L.-T. Phang, *J. Organomet. Chem.*, **381** (1990) 121.
- [3] H.S.O. Chan, T.S. Andy Hor, L.-T. Phang and K.L. Tan, *J. Organomet. Chem.*, **407** (1991) 353.
- [4] T.-J. Kim, S.-C. Kwon, Y.H. Kim, N.H. Heo, M.M. Teeter and A. Yamano, *J. Organomet. Chem.*, **426** (1992) 71.
- [5] L.-T. Phang, K.-S. Gan, H.K. Leo and T.S. Andy Hor, *J. Chem. Soc., Dalton Trans.*, (1993) 2697.
- [6] T.S. Andy Hor, H.S.O. Chan, L.-T. Phang, Y.K. Yan, L.-K. Liu and Y.-S. Wen, *Polyhedron*, **10** (1991) 2437.
- [7] Y.K. Yan, H.S.O. Chan, T.S. Andy Hor, K.L. Tan, L.-K. Liu and Y.-S. Wen, *J. Chem. Soc., Dalton Trans.*, (1992) 423.
- [8] E. Cramer and V. Percec, *Polym. Prepr., Am. Chem. Soc., Div. Polym. Chem.*, **31** (1990) 516.
- [9] T.-J. Kim, K.-H. Kwon, S.-C. Kwon, J.-O. Baeg, S.-C. Shim and D.-H. Lee, *J. Organomet. Chem.*, **389** (1990) 205.
- [10] M. Sato, H. Shigeta, M. Sekino and S. Akabori, *J. Organomet. Chem.*, **458** (1993) 199.
- [11] V. Munyejabo, J. Damiano, M. Postel, C. Bensimon and J.L.A. Rouston, *J. Organomet. Chem.*, **491** (1995) 61.
- [12] T.S. Andy Hor, S.P. Neo, C.S. Tan, T.C.W. Mak, K.W.P. Leung and R.-J. Wang, *Inorg. Chem.*, **31** (1992) 4510.
- [13] T. Cuvigny and M. Julia, *J. Organomet. Chem.*, **317** (1986) 383.

- [14] W.R. Cullen, T.-J. Kim, F.W.B. Einstein and T. Jones, *Organometallics*, 4 (1985) 346.
- [15] N. Miyaara, T. Ishiyama, H. Sasaki, M. Ishikawa, M. Satoh and A. Suzuki, *J. Am. Chem. Soc.*, 111 (1989) 314.
- [16] K. Yuan and W.J. Scott, *Tetrahedron Lett.*, 32 (1991) 189.
- [17] P.L. Castle and D.A. Widdowson, *Tetrahedron Lett.*, 27 (1986) 6013.
- [18] G. Marr and B.W. Rockett, *J. Organomet. Chem.*, 392 (1990) 93.
- [19] A. Houlton, R.M.G. Roberts, J. Silver and R.V. Parish, *J. Organomet. Chem.*, 418 (1991) 269.
- [20] C.E. Housecroft, S.M. Owen, P.R. Raithby and B.A.M. Shaykh, *Organometallics*, 9 (1990) 1617.
- [21] W.H. Watson, A. Nagl, S. Hwang and M.G. Richmond, *J. Organomet. Chem.*, 445 (1993) 163.
- [22] J.H. Enemark and R.D. Feltham, *Coord. Chem. Rev.*, 13 (1974) 339.
- [23] R.D. Feltham, *Inorg. Synth.*, 16 (1975) 1.
- [24] E. Leroy, D. Huchette, A. Mortreux and F. Petit, *Nouv. J. Chim.*, 4 (1980) 173.
- [25] I. Tkatchenko, *J. Mol. Catal.*, 4 (1978) 163.
- [26] D. Ballivet and I. Tkatchenko, *J. Mol. Catal.*, 1 (1975) 319.
- [27] A. Mortreux and F. Petit, *Appl. Catal.*, 24 (1986) 1.
- [28] K.K. Pandey, *Coord. Chem. Rev.*, 51 (1983) 69.
- [29] D. Ballivet, C. Billard and I. Tkatchenko, *Inorg. Chim. Acta*, 25 (1977) L58.
- [30] D. Huchette, J. Nicole and F. Petit, *Tetrahedron Lett.*, (1979) 1035.
- [31] A.R. Butler and D.L.H. Williams, *Chem. Soc. Rev.*, (1993) 233.
- [32] R.L. Keiter, E.A. Keiter, K.H. Hecker and C.A. Boecker, *Organometallics*, 7 (1988) 2466.
- [33] A.E. Gerbase, R.F.d. Souza, E.J.S. Vichi and F.O.V. Cunha, *Angew. Makrom. Chem.*, 239 (1996) 33.
- [34] S.D. Ittel, C.A. Tolman, P.J. Krusic, A.D. English and J.P. Jesson, *Inorg. Chem.*, 17 (1978) 3432.
- [35] D. Ballivet and I. Tkatchenko, *Inorg. Chem.*, 16 (1977) 945.
- [36] D. Ballivet-Tkatchenko, C. Billard and A. Revillon, *J. Poly. Sci., Poly. Chem. Ed.*, 19 (1981) 1697.
- [37] CAD4, automatic four circle diffractometer, Enraf-Nonius, Delft, Netherlands, 1992.
- [38] Structure Determination Package VAXSDP, Version 3.0, B.A. Frenz and Associates Inc., College Station, TX and Enraf-Nonius Delft, Netherlands, 1986.
- [39] G.M. Sheldrick, SHELXS86, program for crystal structure solution, University of Göttingen, Germany, 1990.
- [40] G.M. Sheldrick, SHELXS93, program for crystal structure solution, University of Göttingen, Germany, 1993.
- [41] N. Walker and D. Stuart, *Acta Crystallogr., Sect. A*, 39 (1983) 158.
- [42] S. Bhaduri, K. Grundy and B.J.G. Johnson, *J. Chem. Soc., Dalton Trans.*, (1977) 2085.
- [43] J.J. Bishop, A. Davison, M.L. Katcher, D.W. Lichtenberg, R.E. Merrill and J.C. Smart, *J. Organomet. Chem.*, 27 (1971) 241.
- [44] B. Corain, B. Longato, G. Favero, D. Ajo, G. Pilloni, U. Russo and F.R. Kreissl, *Inorg. Chim. Acta*, 157 (1989) 259.
- [45] P.E. Garrou, *Chem. Rev.*, 81 (1981) 229.
- [46] C.K. Johnson, ORTEP, a thermal-ellipsoid plot program, Oak Ridge National Laboratory, TN, 1965.
- [47] R.D. Feltham and J.H. Enemark, *Top. Stereochem.*, 12 (1981) 155.
- [48] M. Postel, M. Pierrot and H.L.K. Wah, *Inorg. Chim. Acta*, 165 (1989) 215.
- [49] J.A. Kaduk and J.A. Ibers, *Inorg. Chem.*, 16 (1977) 3283.
- [50] R.L. Martin and D. Taylor, *Inorg. Chem.*, 15 (1976) 2970.
- [51] A. Houlton, S.K. Ibrahim, J.R. Dilworth and J. Silver, *J. Chem. Soc., Dalton Trans.*, (1990) 2421.
- [52] J.P. Crow, W.R. Cullen, F.G. Herring, J.R. Sams and R.L. Tapping, *Inorg. Chem.*, 10 (1971) 1616.
- [53] H. Mosbaek and K.G. Poulsen, *Acta Chem. Scand., Ser. A*, 28 (1974) 157.
- [54] N.N. Greenwood and T.C. Gibb, *Mössbauer Spectroscopy*, Chapman and Hall, London, 1971.
- [55] R. Seeber, G. Albertin and G.A. Mazzochin, *J. Chem. Soc., Dalton Trans.*, (1982) 2561.
- [56] L. Ramaley and J. Krause, *Anal. Chem.*, 41 (1969) 1362.
- [57] J.J. O'Dea, J. Osteryoung and R.A. Osteryoung, *Anal. Chem.*, 53 (1981) 695.
- [58] J. Heinze, *Angew. Chem., Int. Ed. Engl.*, 23 (1984) 831.
- [59] S.W. Blanch, A.M. Bond and R. Colton, *Inorg. Chem.*, 20 (1981) 755.
- [60] P.K. Baker, N.G. Connelly, B.M.R. Jones, J.P. Maher and K.R. Somers, *J. Chem. Soc., Dalton Trans.*, (1980) 579.
- [61] H.W. Chen and W.J. Jolly, *Inorg. Chem.*, 18 (1979) 2549.
- [62] P.K. Baker, K. Broadley and N.G. Connelly, *J. Chem. Soc., Dalton Trans.*, (1982) 471.
- [63] G. Pilloni, B. Longato and B. Corain, *J. Organomet. Chem.*, 420 (1991) 57.
- [64] C. Vogler and W. Kaim, *J. Organomet. Chem.*, 398 (1990) 293.
- [65] L.-T. Phang, S.C.F. Au-Yeung, T.S. Andy Hor, S.B. Khoo, Z.-Y. Zhou and T.C.W. Mak, *J. Chem. Soc., Dalton Trans.*, (1993) 165.
- [66] G. Pilloni and B. Longato, *Inorg. Chim. Acta*, 208 (1993) 17.
- [67] T.M. Miller, K.J. Ahmed and M.S. Wrighton, *Inorg. Chem.*, 28 (1989) 2347.
- [68] P. Seiler and J.D. Dunitz, *Acta Crystallogr., Sect. B*, 35 (1979) 1068.
- [69] M.R. Churchill, A.G. Lander and A.L. Rheingold, *Inorg. Chem.*, 20 (1981) 849.
- [70] S.J. Gelb, A.L. Rheingold, T.Y. Dong and D.N. Heindrickson, *J. Organomet. Chem.*, 312 (1986) 241.
- [71] A. Cinquantini, G. Opromola, P.F. Zanello and G. Giorgi, *J. Organomet. Chem.*, 444 (1993) 179, and Refs. therein.